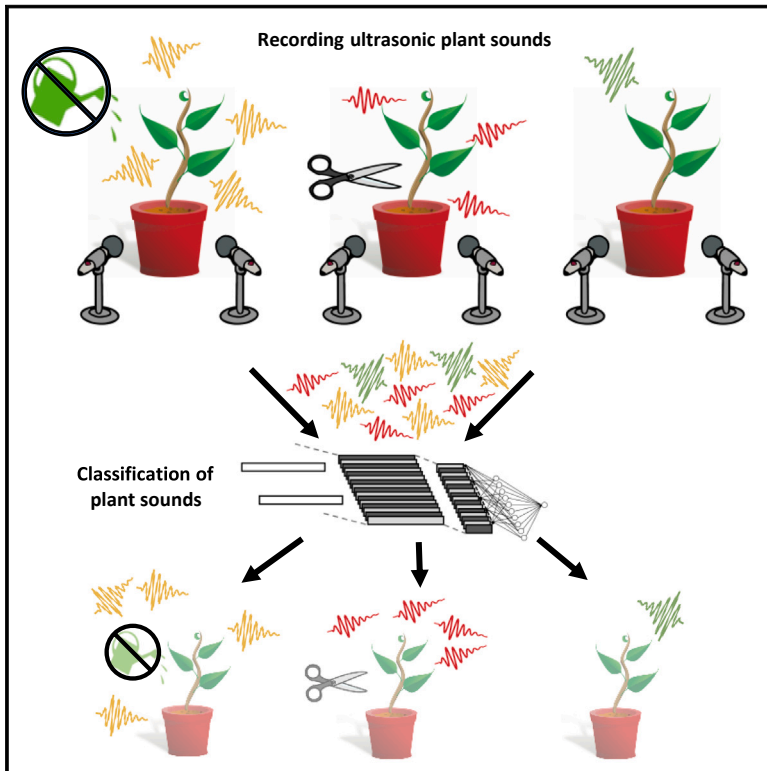


# Sounds emitted by plants under stress are airborne and informative

## Graphical abstract



## Authors

Itzhak Khait, Ohad Lewin-Epstein, Raz Sharon, ..., Nir Sade, Yossi Yovel, Lilach Hadany

## Correspondence

lilach.hadany@gmail.com

## In brief

Plants emit species- and stress-specific airborne sounds that can be detected in acoustic chambers and greenhouses.

## Highlights

- Plants emit ultrasonic airborne sounds when stressed
- The emitted sounds reveal plant type and condition
- Plant sounds can be detected and interpreted in a greenhouse setting



Article

# Sounds emitted by plants under stress are airborne and informative

Itzhak Khait,<sup>1,6,9</sup> Ohad Lewin-Epstein,<sup>1,7,8,9</sup> Raz Sharon,<sup>1,2</sup> Kfir Saban,<sup>1</sup> Revital Goldstein,<sup>1</sup> Yehuda Anikster,<sup>1</sup> Yarden Zeron,<sup>1</sup> Chen Agassy,<sup>1</sup> Shaked Nizan,<sup>1</sup> Gayl Sharabi,<sup>1</sup> Ran Perelman,<sup>1</sup> Arjan Boonman,<sup>3</sup> Nir Sade,<sup>1,4</sup> Yossi Yovel,<sup>3,5,10</sup> and Lilach Hadany<sup>1,5,10,11,\*</sup>

<sup>1</sup>School of Plant Sciences and Food Security, Tel-Aviv University, Tel-Aviv, Israel

<sup>2</sup>School of Mathematical Sciences, Tel-Aviv University, Tel-Aviv, Israel

<sup>3</sup>School of Zoology, Tel-Aviv University, Tel-Aviv, Israel

<sup>4</sup>The Institute of Cereal Crop Improvement, Tel Aviv University, Tel Aviv, Israel

<sup>5</sup>Sagol School of Neuroscience, Tel Aviv University, Tel-Aviv, Israel

<sup>6</sup>Present address: Centure Applications (Greeneye Technology), Tel Aviv, Israel

<sup>7</sup>Present address: Broad Institute of MIT and Harvard, Cambridge, MA, USA

<sup>8</sup>Present address: Center for Computational and Integrative Biology, Massachusetts General Hospital and Harvard Medical School, Boston, MA, USA

<sup>9</sup>These authors contributed equally

<sup>10</sup>These authors contributed equally

<sup>11</sup>Lead contact

\*Correspondence: [lilach.hadany@gmail.com](mailto:lilach.hadany@gmail.com)

<https://doi.org/10.1016/j.cell.2023.03.009>

## SUMMARY

**Stressed plants show altered phenotypes, including changes in color, smell, and shape. Yet, airborne sounds emitted by stressed plants have not been investigated before. Here we show that stressed plants emit airborne sounds that can be recorded from a distance and classified. We recorded ultrasonic sounds emitted by tomato and tobacco plants inside an acoustic chamber, and in a greenhouse, while monitoring the plant's physiological parameters. We developed machine learning models that succeeded in identifying the condition of the plants, including dehydration level and injury, based solely on the emitted sounds. These informative sounds may also be detectable by other organisms. This work opens avenues for understanding plants and their interactions with the environment and may have significant impact on agriculture.**

## INTRODUCTION

Plants exhibit significant changes in their phenotypes in response to stress. They differ visually, with respect to both color and shape, from unstressed plants.<sup>1–4</sup> They also emit volatile organic compounds (VOCs), e.g. when exposed to drought or herbivores.<sup>5,6</sup> VOCs can also affect neighboring plants, resulting in increased resistance in these plants.<sup>7,8</sup> Altogether, plants have been demonstrated to produce visual, chemical, and tactile cues, which other organisms can respond to.<sup>9–12</sup> Nevertheless, the ability of plants to emit airborne sounds—that could potentially be heard by other organisms—has not been sufficiently explored.<sup>11,13,14</sup>

Plant vibrations have been described in several scenarios. Plants exposed to drought stress have been shown to experience cavitation – a process where air bubbles form, expand and collapse in the xylem, causing vibrations.<sup>15,16</sup> These vibrations have been recorded by connecting the recording device directly to the plant.<sup>16–20</sup> Such contact recordings do not reveal the extent to which these (and other) vibrations could result in acoustic emissions that may be detected at a distance from

the plant, if at all.<sup>17,21,22</sup> Thus, the question of airborne sound emission by plants remains unanswered.<sup>17,23,24</sup>

Many animals, including herbivores and their predators, respond to sound.<sup>25–27</sup> Recently, plants were also demonstrated to respond to sounds,<sup>13,28–30</sup> e.g., by changing the expression of specific genes,<sup>29,30</sup> or by increasing sugar concentration in their nectar.<sup>31</sup> Thus, if plants emit airborne sounds, these sounds can potentially trigger a rapid response in nearby organisms, including both animals and plants. Even if the emission of the sounds is merely a result of the plant's physiological condition, nearby organisms that are capable of hearing these sounds could use them for their own benefit. We therefore set to examine whether plants emit informative airborne sounds, which may serve as potential signals or cues to their environment. Here we show that plants indeed emit *airborne* sounds, which can be detected from several meters away, both in acoustic chambers and in greenhouses. Moreover, we show that the emitted sounds carry information about the physiological state of the plant. By training machine learning models, we were able to distinguish between drought-stressed, cut, and control plants, based only on the sounds they emit. These results demonstrate



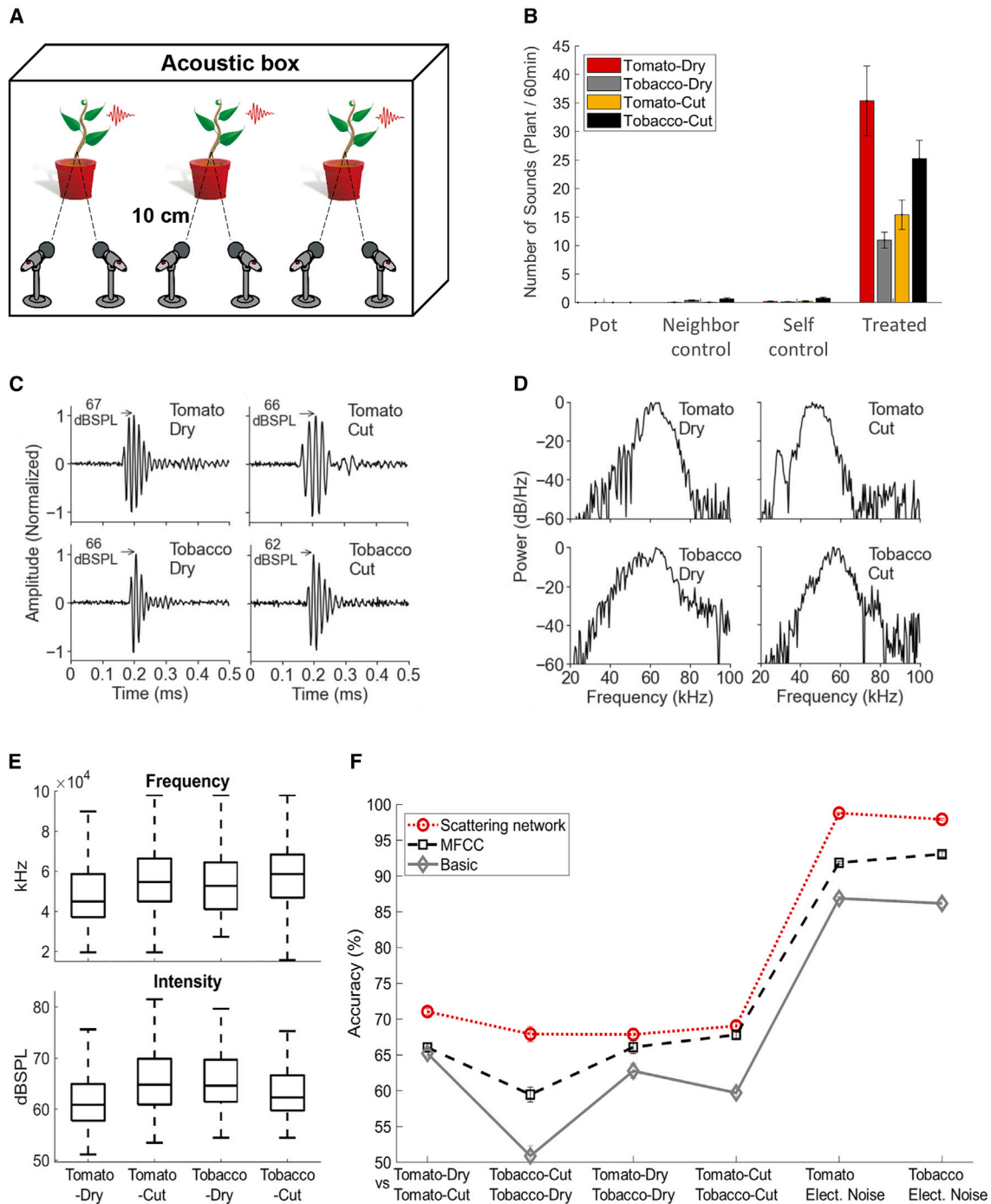


**Figure 1. Stressed plants emit remotely detectable ultrasounds that reveal plant condition and species**

(A) Acoustic box setup. In each recording, three plants are placed inside a  $50 \times 100 \times 150 \text{ cm}^3$  acoustic box with two directional microphones oriented at each plant. Using two microphones helps eliminating false detections resulting from electrical noise of the recording system and cross-plant interference.

(B) Mean number of sounds emitted during 1 h of recording by tomato and tobacco plants under two treatments: drought stress and cutting. Three control groups were used: pot—pots with soil but without a plant; self-control—plant before treatment; and neighbor-control—untreated plants that shared the acoustic box with treated plants. All treatment groups emitted significantly more sounds than all control groups ( $p < e-6$ , Wilcoxon test with Bonferroni correction); less than 1 detection/hour for all plant-treatment combinations in the self-control and neighbor-control groups,  $19 \leq n \leq 51$  plants for each group, and no sound detection in the pot-control group ( $>500$  recording hours). Error bars represent standard errors.

(C) Examples of time signals of sounds emitted by: a drought-stressed tomato, a drought-stressed tobacco, a cut tomato, and a cut tobacco, normalized. Peak dB SPL values at 10 cms, relative to  $20 \mu\text{Pa}$ , are noted by the arrows (see STAR Methods).

(legend continued on next page)

the potential in studying plant bioacoustics, suggest that plant acoustic emissions may play an important role in ecology and evolution, and may have direct implications for plant monitoring in agriculture.

## RESULTS

To investigate plants' airborne sound emissions, we constructed a reliable recording system, where each plant is recorded simultaneously by two microphones (see [Figure 1A](#) for illustration, and [STAR Methods](#) for details). First, we recorded plants within an acoustic box and developed machine learning algorithms to classify the recorded sounds. Then we tested the system in a greenhouse, while monitoring physiological parameters of the recorded plants.

### Stressed plants emit airborne sounds that reveal their condition: Acoustic box setup

We recorded tomato (*Solanum lycopersicum*) and tobacco (*Nicotiana tabacum*) plants under different treatments—drought stress, cutting (of the stem, before recording), and controls, within an acoustically isolated box. We focused on the ultrasonic sound range (20–150 kHz).

We found that plants emit sounds, and that stressed plants—both drought-stressed (*Dry*) and cut plants (*Cut*; see [STAR Methods](#))—emit significantly more sounds than plants of any of the control groups ( $p < e-6$ , Wilcoxon test for each of the 12 comparisons with Holm-Bonferroni correction). Three controls were used for each plant species and treatment: recording from the same plant before treatment (*Self-control*), recording from an untreated same-species neighbor plant (*Neighbor-control*), and recording a pot with soil but without a plant (*Pot*; see [STAR Methods](#)). The mean number of sounds emitted by dry plants was  $35.4 \pm 6.1$  and  $11.0 \pm 1.4$  per hour for tomato and tobacco, respectively, and cut tomato and tobacco plants emitted  $25.2 \pm 3.2$  and  $15.2 \pm 2.6$  sounds per hour, respectively ([Figure 1B](#)). In contrast, the mean number of sounds emitted by plants from all the control groups was lower than 1 per hour. Our system did not record any sound in the *Pot* control ([Figure 1B](#)) over >500 h of recordings.

What does a stressed plant sound like? [Figures 1C](#) and [1D](#) show examples of raw recorded time signals and their spectra as recorded from drought-stressed and cut plants, while the distributions of sound peak intensity and the maximum energy frequency of drought-stressed and cut plants are shown at [Figure 1E](#). The mean peak sound intensity recorded from dry plants was  $61.6 \pm 0.1$  dB SPL and  $65.6 \pm 0.4$  dB SPL at

10 cm, for tomato and tobacco, respectively, and the mean peak frequencies (frequency with maximal energy) of these sounds was  $49.6 \pm 0.4$  kHz and  $54.8 \pm 1.1$  kHz, respectively. The mean peak intensity of the sounds emitted by cut plants was  $65.6 \pm 0.2$  dB SPL and  $63.3 \pm 0.2$  dB SPL at 10.0 cm, for tomato and tobacco, respectively, and the mean peak frequency was  $57.3 \pm 0.7$  kHz and  $57.8 \pm 0.7$  kHz, respectively. Note that due to the directionality of the microphone, this is a lower bound of the intensity (see [STAR Methods](#)).

Spectrograms of raw recorded sounds from drought-stressed and cut plants are shown at [Figure S1A](#), the mean spectra of the sounds are shown in [Figure S1B](#), and an example of the electronic noise is in [Figure S1C](#). An audio sample of the actual tomato recordings, after down sampling to the audible range and condensation in time, is included in [Audio S1](#).

We trained machine learning models to classify different plant conditions and species based on their sound emissions. We divided the sounds into four groups, corresponding to the four combinations of two plant types (tomato or tobacco), and two treatments (drought stress or cutting). A binary classifier was trained to distinguish between two equal-size groups (“pair”) in each comparison (Tomato-Dry vs. Tomato-Cut; Tobacco-Dry vs. Tobacco-Cut; Tomato-Dry vs. Tobacco-Dry; Tomato-Cut vs. Tobacco-Cut). For cross validation, the model was tested only on plants that were not a part of the training process (see [STAR Methods](#) for more details). We used a support vector machine (SVM) as the classifier with several methods of feature extraction—basic,<sup>32,33</sup> MFCC,<sup>34</sup> and a scattering network.<sup>26</sup>

The SVM classifier with scattering network for feature extraction achieved ~70% accuracy for each of the four pairs ([Figure 1F](#) red line), significantly better than random ( $p < e-12$  for each pair, Wilcoxon rank-sum test with Holm-Bonferroni correction). The same classifier was trained to discriminate between the electrical noise of the system (see [STAR Methods](#)) and the sounds emitted by the plants (Tomato vs. Noise, Tobacco vs. Noise) and achieved above 98% accuracy for both ([Figure 1F](#)). The results were also robust to the dimension of the descriptors and the scattering network specific parameters ([Figure S1D](#)). When using the SVM classifier with MFCC as the input features, the results were still significantly better than random (black line,  $p < e-4$  for each pair, corrected as above), and even when using only 4 “basic” features (see [STAR Methods](#)), the results were significantly better than random for 5 of the 6 pairs ( $p < e-6$  for each of them, adjusted; [Figure 1F](#) gray line). However, scattering network performed better than either MFCC or Basic for all the pairs ( $p < 0.05$  and  $p < e-6$ , respectively; Wilcoxon signed-rank test). Altogether, these results demonstrate that plant

(D) The normalized spectra of the sounds from (C).

(E) The recorded sounds intensity peak and the max energy frequency for the four groups—drought-stressed tomato plants, cut tomato plants, drought-stressed tobacco plants, and cut tobacco plants.

(F) The accuracy of sound classification achieved by different feature extraction methods, with an SVM classifier. The best results were obtained using the scattering network method for feature extraction (red line,  $p < e-12$  for each pair). Using MFCC for feature extraction the results were also highly significant (black dashed line,  $p < e-4$  for each pair) and even basic methods for feature extraction allowed for better-than-random classification (gray line,  $p < e-6$  for each pair apart from one case: Tobacco dry vs. Tobacco cut, which was not significant with the basic method). The comparisons Tomato vs. Elect. Noise and Tobacco vs. Elect. Noise refer to electrical noise of the recording system. Training set size of the two groups in each pair was equal (400 < sounds for each pair, see [Table S1](#)), and significance levels for each pair were calculated using Wilcoxon rank-sum test with Holm-Bonferroni correction for multiple comparisons. Error bars represent standard deviations. The classification results were reproduced using CNN models (see [STAR Methods](#) and [Figure S1E](#)).

See also [Figure S1](#).

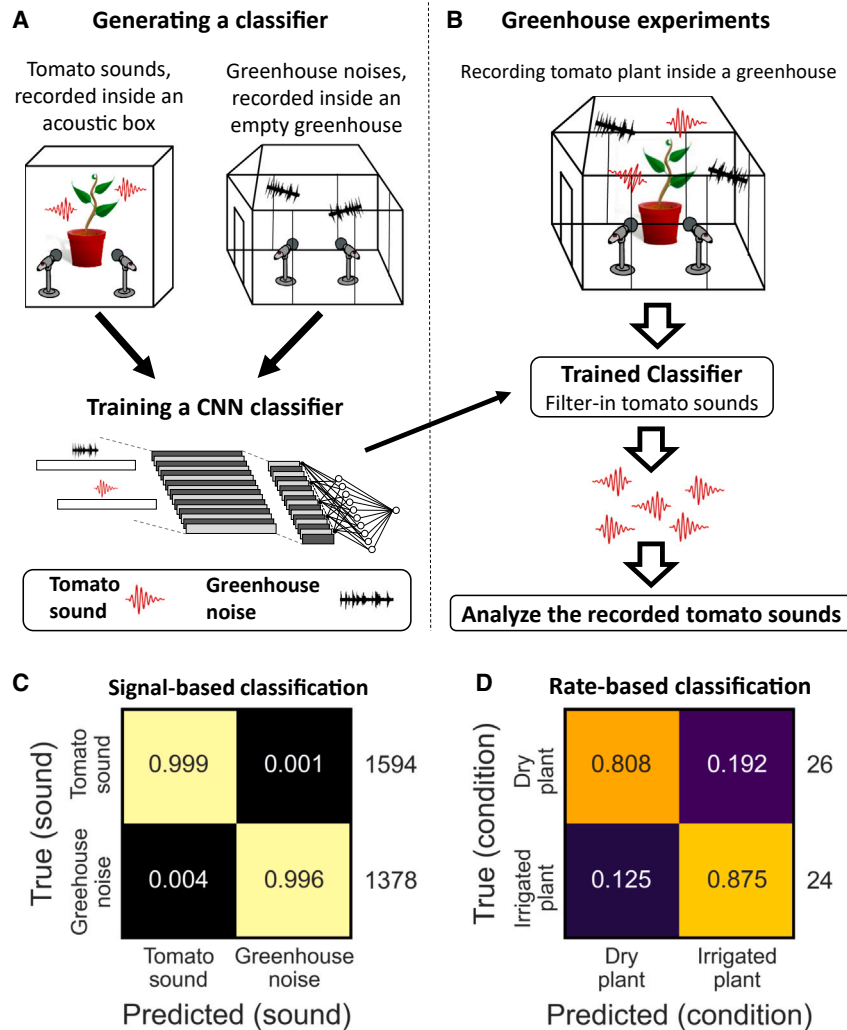


**Figure 2. Acoustic detection of plant condition in the greenhouse**

(A) Illustration of the procedure used to train a classifier that distinguishes between tomato sounds and greenhouse noises. A background noises library was first generated, by recording inside an empty greenhouse for several days. Using this library and the library of tomato sounds recorded in an acoustic box, we trained a convolution neural network (CNN) classifier to distinguish between tomato sounds and background noises.

(B) Illustration of the recordings in the greenhouse. Tomato plants were recorded in the greenhouse. The recorded sounds were filtered using the trained CNN classifier, leaving only the sounds classified as tomato sounds.

(C) Confusion matrix showing the success of trained CNN classifiers in distinguishing between tomato sounds and background noises in a cross-validation examination (see STAR Methods). Balanced accuracy score of 99.7%.

(D) Confusion matrix showing the success in distinguishing between dry and irrigated tomato plants, based on 1 h of recording in the greenhouse. The condition of the plant (dry/irrigated) was determined based on the number of recorded sounds classified as tomato sounds: if above three, the plant was classified as “dry”, and otherwise as “irrigated”. Balanced accuracy score of 84% ( $p < e-5$ ; Fisher exact test).

See also Figure S2.

sounds carry information that can be interpreted and used for classification of plant type and condition.

### Plant stress can be identified from its sounds in a greenhouse

We also tested the acoustic behavior of plants in a greenhouse, in the presence of many background noises that were absent in the acoustic box (e.g. wind, air-conditioning, maintenance work). In order to distinguish between the sounds generated by plants and background greenhouse noises, we first constructed a library of greenhouse noises, by recording in an empty greenhouse. We then trained a convolution neural network (CNN) model to distinguish between these empty greenhouse noises and the sounds of dry tomatoes recorded in the acoustic box (Figure 2A; see details in STAR Methods section). The models obtained from this training achieved 99.7% balanced accuracy in a cross-validation examination (Figure 2C). Similarly, significant results were obtained when controlling for sound intensity differences between plant and noise sounds and for the difference in background sounds between the acoustic box and the

greenhouse (see “classifying sounds in the greenhouse” in the STAR Methods and Figures S2A and S2B for details). We then trained a model on the entire datasets (empty greenhouse noises and dry tomato sounds from the acoustic box) and applied it to another set of recordings of tomatoes in the greenhouse. After filtering out the background noises based on our model’s classification, the number of plant sounds per hour of recording was highly indicative of the plant’s condition, distinguishing drought-stressed plants from control plants with ~84% accuracy ( $p < e-5$ , Fisher exact test; see Figures 2B and 2D and further details in Figures S2C and S2D).

We then tested the acoustic manifestation of the dehydration process by recording 23 tomato plants for several consecutive days without watering. We recorded in the greenhouse while monitoring soil moisture in each pot and paired each recorded sound with the volumetric water content (VWC) measurement of the recorded plant at the time of recording. We used the CNN model mentioned above (Figures 2A and 2B) to separate tomato sounds from background noises and monitored the number of tomato-classified sounds recorded from each plant. The results revealed a clear temporal acoustic pattern: the plants emit very few sounds when irrigated, the number of sounds per day increases in the following 4–5 days, and then the number of sounds decreases as the plant dries up (Figure 3A). The number of emitted sounds showed a bimodal pattern along the day:

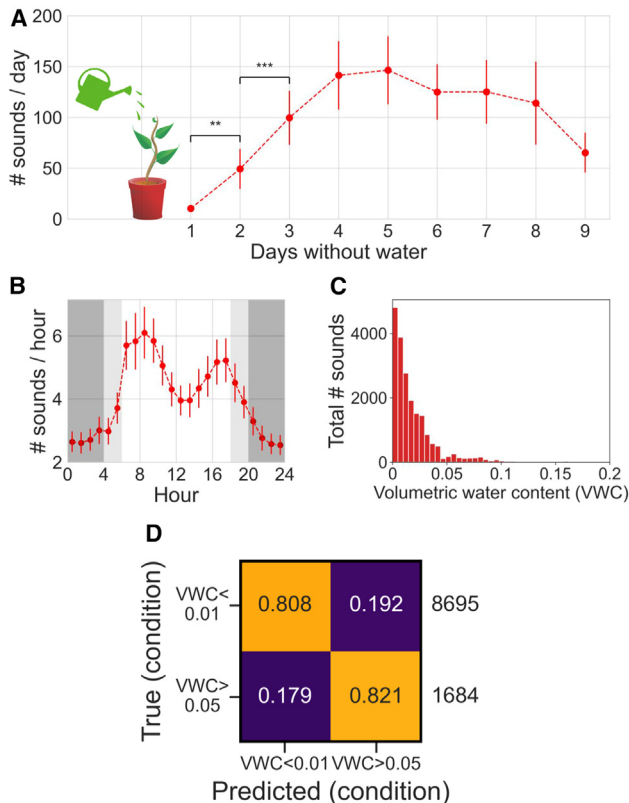


**Figure 3. Acoustic manifestation of dehydration in tomato plants as observed in long-term recordings in a greenhouse**

23 tomato plants were recorded inside a greenhouse for nine consecutive days after watering, and the volumetric water content (VWC) of their soil was measured throughout the experiment. The recorded sounds were filtered using the trained CNN classifier, leaving only the sounds classified as emitted by tomatoes.

(A) The number of sounds per day along nine consecutive days of dehydration. The dots represent the average of 23 plants, while the error bars represent the standard errors. We find significant differences in the number of emitted sounds between the first and second day, and between the second and third day ( $p$  values are  $<0.01$  and  $<0.001$ , respectively;  $p$  values were calculated using Wilcoxon signed-rank tests, adjusted for 8 comparisons between pairs of consecutive days using Holm-Bonferroni method). The soil VWC of the plants at the beginning of the recording was  $0.21 \pm 0.03$  ( $m^3/m^3$ ).

(B) The number of sounds per hour is plotted as function of the time of day. Each dot represents the average number of sounds emitted in the relevant hour over all 23 plants and nine days for each plant, while the error bars represent the standard errors. Dark gray areas represent the hours of complete darkness, light gray areas show when the greenhouse lighting was on, and the white area represents the approximate hours of natural daylight.

(C) A histogram showing the total number of emitted sounds as function of the plant VWC during sound emission. Out of all the emitted plant sounds in this experiment (over 20,000 sounds),  $\sim 92\%$  were emitted when  $VWC \leq 0.05$ , and  $\sim 43\%$  when  $VWC \leq 0.01$ . To correct for variability between plants, we repeated the analyses of (A–C) while normalizing the sounds of each plant by the overall number of sounds it emitted throughout the experiment, and found very similar results (see Figures S3A–S3C).

(D) Confusion matrix showing the success of the trained CNN classifier in distinguishing between individual sounds emitted by a plant experiencing  $VWC < 0.01$  and sounds emitted by a plant experiencing  $VWC > 0.05$ . This classification achieved balanced accuracy score of 81% (average of leave-one-plant-out cross validation; see STAR Methods).

See also Figure S3.

one major peak in the morning hours, 08:00–12:00; and a second smaller peak in the afternoon, 16:00–19:00 (Figure 3B). Such “midday depression” has previously been observed with respect to stomatal conductance,<sup>35,36</sup> suggesting that the two processes may be associated. We also found a strong association between the VWC of the soil and plant sound emission. Consistent with our results from the acoustic box (Figure 1B), we found that the vast majority of the plant sounds are emitted when the VWC is  $<0.05$ , and almost no sounds are emitted when the VWC is  $>0.1$  (Figure 3C). Repeating the analysis presented in Figures 3A–3C controlling for the individual variation in the number of sounds emitted by different plants resulted in very similar results (Figures S3A–S3C).

We further examined whether the plants emitted different sounds at different levels of dehydration. We divided the sounds that were recorded in the experiment and classified as tomato sounds into two groups according to the VWC of the plant at the time of the sound emission:  $VWC < 0.01$  and  $VWC > 0.05$ . We then trained CNN models to distinguish between the groups according to the sound and achieved 81% balanced accuracy in a cross-validation examination (see STAR Methods) (Figure 3D). Classification of sounds grouped to  $VWC < 0.05$  and  $VWC > 0.05$  yielded  $>72\%$  balanced accuracy (Figure S3D). We conducted a second analysis of the sounds recorded in that greenhouse experiment, without pre-classification of the sounds to tomato sounds and background noises. Here we defined three groups of sounds: all sounds from the greenhouse experiment that were associated with plant VWC lower than 0.01; all sounds from the greenhouse experiment that were associated with plant VWC greater than 0.05; and the library of empty greenhouse noises. We trained CNN models to distinguish between the sounds of these three groups. The results of this classification were still highly significant (balanced accuracy  $>75\%$ ), even with normalized sound intensity (Figure S3E).

To investigate the generality of our results, we also performed a small survey of different plant species. We successfully recorded sounds from additional plants from different taxa, including *Triticum aestivum* (wheat), *Zea mays* (corn), *Vitis vinifera* (Cabernet Sauvignon grapevine), *Mammillaria spinosissima* (pincushion cactus) and *Lamium amplexicaule* (henbit) (see Figure S3F), but not from woody parts of almond and grapevine. We thus expect that many plants emit sounds, but the diversity of characteristics of these sounds are yet to be researched. We have also successfully recorded tomato plants under a different stress—infection with TMV (Figure S3F). We thus expect that many plants emit sounds under different stresses, but the diversity of characteristics of these sounds are yet to be researched.

Finally, we investigated the correlation between the emitted sounds and the physiological state of tomato plants, focusing on the transpiration rate patterns during drought. We monitored plants in the greenhouse for several consecutive days without watering and collected the hourly number of emitted sounds as well as the hourly average transpiration rate of each plant, using plant-DiTech system (see STAR Methods). We found a strong correlation between the number of sounds emitted per hour and the corresponding transpiration rate of the plant, with a similar trend of low values during night-time, and a peak in

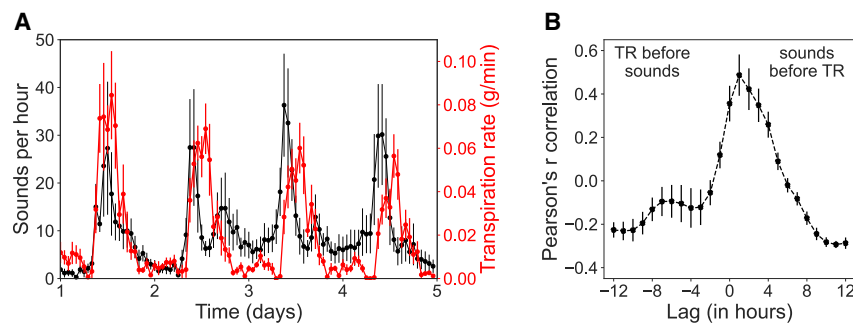


**Figure 4. Plant sounds correlate with the transpiration rate**

The sounds and transpiration rates (TR) of seven tomato plants were monitored for several days without watering.

(A) The number of tomato sounds per hour (black) and the hourly TR (red) are plotted along the four consecutive days in which each plant made the most sounds. Each dot represents the average of seven plants, with the bars presenting the standard errors.

(B) Cross-correlation plot. Pearson's R correlation coefficient between the hourly mean number of sounds and the hourly mean TR is plotted (y axis) as

a function of the time lag (in hours) between the timing of the sounds and the TR (x axis). Each dot represents the average correlation across all seven plants for the lag specified in the x axis, while the bars represent the standard errors.

See also Figure S4.

the late morning-noon time. Nevertheless, we see that the daily transpiration rate decreases as dehydration continues, while the number of emitted sounds does not (Figure 4).

## DISCUSSION

Our results demonstrate that plants emit remotely detectable and informative airborne sounds under stress (Figure 1). The plant emissions that we report, in the ultrasonic range of ~20–100 kHz, could be detected from a distance of 3–5 m, by many mammals and insects (given their hearing sensitivity, e.g., mice<sup>37</sup> and moths<sup>27,38</sup>; see STAR Methods for details on the estimation of animal detection ranges). We succeeded in differentiating between sounds emitted under two different stress conditions—dry and cut plants—with an accuracy of 70% using supervised machine learning methods (Figure 1), and distinguishing between drought-stressed and control plants in a greenhouse, based only on the sounds they emit (accuracy of 84%, Figures 2B and 2D). We monitored the distribution of plant sounds with respect to days of dehydration, time of day, soil moisture (Figure 3), and transpiration rate (Figure 4). Our recordings revealed that the hourly pattern of sound emission correlates with the plant's transpiration rate, while the daily number of sounds is a hump-shaped function of plant dehydration, increasing during the first days of dehydration, and declining as the plant dries up. The sounds emitted by the plants at high and low levels of dehydration are different, and we succeeded classifying them with an accuracy of 81% (Figure 3). These findings can alter the way we think about the plant kingdom, which has been considered to be almost silent until now.<sup>23</sup>

One potential mechanism that may be responsible for the emission of at least part of the sounds we record is cavitation in the stem.<sup>16</sup> Several findings support this: (1) we found that the frequencies of the sounds emitted by different plant species correspond to their trachea diameter, with wider tracheas in the plants emitting lower sounds (Figures S4A and S4B), consistent with the observed negative association between xylem diameter and resonance frequency.<sup>39</sup> (2) The different sounds emitted under drying and cutting (Figure 1) are in accordance with the different gas dynamics of the plant in these two processes: while drying is gradual, with a low rate of air-seeding and reduced pressure, cutting involves a rapid and significant air-seeding

through all the trachea in the cut stem. In accordance, sounds were emitted by cut plants for a shorter period of time than by dry plants. Of the sounds emitted by plants that were both cut and dry, the majority were classified as “cut” in the first day, but the picture is reversed in the following days, with a majority of sounds classified as “dry” (Figure S4C). (3) A 3D acoustic simulation shows that sounds emitted from the trachea would radiate from the stem in all directions (Figure S4D). This is consistent with the results of our two-microphone recording system, which picked up sound on two sides of the stem they were directed to (Figure 1A). (4) The frequency range of cavitation-related vibrations partially overlaps with the sounds we recorded.<sup>17</sup> When recorded with contact sensors, cavitation is usually also characterized by additional higher frequencies that are beyond the sensitivity range of our microphones and that would attenuate rapidly in air. Yet, only the vibrations that result in airborne sounds (which we report here) are the ones that have a potential of affecting other organisms and human-sensors that are not in direct contact with the plant. When considering groups of plants, the advantage of tracking airborne sound may be even greater, as a single artificial sensor for airborne sounds could detect sounds requiring multiple contact sensors.

A potential application of our results can be for monitoring plants in the field or greenhouse.<sup>40</sup> Specifically, plant sound emissions could offer a way for monitoring crops water and possibly disease states—questions of crucial importance in agriculture.<sup>41</sup> More precise irrigation can save up to 50% of the water expenditure and increase the yield, with dramatic economic implications.<sup>41,42</sup> In times when more and more areas are exposed to drought due to climate change,<sup>43</sup> efficient water use becomes even more critical, for both food security and ecology. Our results, demonstrating the ability to distinguish between drought-stressed and control plants based on plant airborne sounds, open an avenue of research in the field of precision agriculture.

We have shown that plant sounds can be effectively classified by machine learning algorithms. We thus suggest that other organisms may have evolved to classify these sounds as well and respond to them. For instance, many moths—some of them using tomato and tobacco as hosts for their larvae<sup>44,45</sup>—can hear and react to ultrasound in the frequencies and intensities that we recorded.<sup>25–27</sup> Nearby plants may also respond to the sounds emitted by plants. Plants were already shown to

react to sounds<sup>13,28–31,46</sup> and specifically to increase their drought tolerance in response to sounds.<sup>47,48</sup> Could plants potentially respond adaptively to the sounds of their drought-stressed or injured neighbors? We suggest that more investigation in the plant bioacoustics field, and particularly in the ability of plants to emit and react to sounds under different conditions and environments, may reveal a pathway of signaling between plants and their environment.

### Limitations of the study

Although our study demonstrates that plants emit informative airborne sounds under stress, there are a few open issues: First, our results were obtained on a limited number of plant species, and should be tested on additional species of plants from different families. In a small survey, we successfully recorded sounds from plants of 5 additional taxa (see Figure S3F). We thus expect that many plants emit sounds, but the diversity of characteristics of these sounds are yet to be identified. Second, future studies could explore the sounds emitted under different conditions. We observed sound emission in plants exposed to drought, cutting, or TMV infection (Figures 1 and S3F). Other potential conditions include different pathogens, cold, herbivores attack, UV radiation, and other life stages of the plant species, such as flowering. Third, our understanding of the sound emission mechanism is still rudimentary. This is an area for future investigation. Finally, our results were obtained in either a controlled acoustic environment (an acoustic chamber) or a semi-natural environment (greenhouse). Recording and analysis of plant sounds in the field, with a wider range of background noises, would present additional challenges.

### STAR★METHODS

Detailed methods are provided in the online version of this paper and include the following:

- KEY RESOURCES TABLE
- RESOURCE AVAILABILITY
  - Lead contact
  - Data and code availability
- EXPERIMENTAL MODEL AND SUBJECT DETAILS
- METHOD DETAILS
  - Recording protocol
  - Data pre-processing
  - Acoustic-box drought stress experiment
  - Acoustic-box cut stress experiment
  - Greenhouse drought experiment
  - Greenhouse dehydration experiment
  - Greenhouse whole plant transpiration rate
  - Classifying sounds recorded in the acoustic box
  - Convolution neural networks (CNN)
  - Leave-one-plant-out cross validation (LOPO-CV)
  - Classifying sounds recorded in the greenhouse
  - Estimation of the animal detection range
  - Microphone calibration
  - Estimating the acoustic box properties
- QUANTIFICATION AND STATISTICAL ANALYSIS

### SUPPLEMENTAL INFORMATION

Supplemental information can be found online at <https://doi.org/10.1016/j.cell.2023.03.009>.

### ACKNOWLEDGMENTS

We thank Daniel Chamovitz, Gal Chechik, Tuvik Beker, Marcus W. Feldman, Judith Berman, and Ella Sklan for comments on the paper; Guido Sessa, Doron Teper, Guy Sobol, Yura Pupov, Rotem Shteinshleifer, Odelia Pisanty, Eilon Shani, Mor Binder, Meirav Leibman-Markus, and Alin Finkelstein for helping with plants materials; Aviv Dombrovsky for TMV; Yoel Shkolnisky, Marine Veits, Ilia Raysin, Uri Obolski, Yoav Ram, Eyal Zinger, Yael Gurevich, Eylon Tamir, Yuval Sapir, Yaara Blogovski, and Ruth Cohen-Khait for comments on the way; Yonatan Bendett for comments and artwork. The Titan Xp used for this research was donated by the NVIDIA Corporation.

**Funding:** The research has been supported in part by Bikura 2308/16 (L.H., Y.Y.), Bikura 2658/18 (L.H., Y.Y.), ISF 2064/18 (L.H.), Tel Aviv University Center for AI and Data Science (TAD) (L.H., Y.Y.), by the Manna Center Program for Food Safety and Security fellowships (I.K.), and by the Clore Foundation Scholars Program (O.L.-E.).

### AUTHOR CONTRIBUTIONS

L.H. and I.K. conceived the study. L.H., Y.Y., I.K., O.L.-E. and N.S. designed the research. I.K., O.L.-E., K.S., R.G., Y.Z., Y.A., S.N., R.P., and G.S. performed the experiments. O.L.-E., R.S., I.K., A.B., Y.A., C.A., and L.H. analyzed the data. L.H., Y.Y., and N.S. supervised the experiments. L.H. and Y.Y. supervised the analysis. I.K. and O.L.-E. contributed equally to the study. L.H. and Y.Y. contributed equally to the study. All authors discussed the results and took part in writing the manuscript.

### DECLARATION OF INTERESTS

Itzhak Khait, Raz Sharon, Yossi Yovel, and Lilach Hadany submitted a patent application related to this work: Plant-monitor. Patent application number WO2020039434A1. (2020). The remaining authors declare no competing interests.

Received: July 27, 2021

Revised: November 29, 2022

Accepted: March 6, 2023

Published: March 30, 2023

### REFERENCES

1. Hsiao, T.C. (1973). Plant responses to water stress. *Annu. Rev. Plant Physiol.* *24*, 519–570.
2. Jackson, R.D. (1986). Remote sensing of biotic and abiotic plant stress. *Annu. Rev. Phytopathol.* *24*, 265–287.
3. Mahlein, A.-K. (2016). Plant disease detection by imaging sensors—parallels and specific demands for precision agriculture and plant phenotyping. *Plant Dis.* *100*, 241–251.
4. Potters, G., Pasternak, T.P., Guisez, Y., Palme, K.J., and Jansen, M.A.K. (2007). Stress-induced morphogenic responses: growing out of trouble? *Trends Plant Sci.* *12*, 98–105.
5. Holopainen, J.K., and Gershenzon, J. (2010). Multiple stress factors and the emission of plant VOCs. *Trends Plant Sci.* *15*, 176–184.
6. Paré, P.W., and Tumlinson, J.H. (1999). Plant volatiles as a defense against insect herbivores. *Plant Physiol.* *121*, 325–332.
7. Heil, M., and Karban, R. (2010). Explaining evolution of plant communication by airborne signals. *Trends Ecol. Evol.* *25*, 137–144.
8. Dolch, R., and Tschamtkke, T. (2000). Defoliation of alders (*Alnus glutinosa*) affects herbivory by leaf beetles on undamaged neighbours. *Oecologia* *125*, 504–511.



9. Karban, R. (2008). Plant behaviour and communication. *Ecol. Lett.* *11*, 727–739.
10. Falik, O., Mordoch, Y., Quansah, L., Fait, A., and Novoplansky, A. (2011). Rumor has it...: relay communication of stress cues in plants. *PLoS One* *6*, e23625. <https://doi.org/10.1371/journal.pone.0023625>.
11. Chamovitz, D. (2012). What a Plant Knows: A Field Guide to the Senses of Your Garden-And beyond (Scientific American/Farrar, Straus and Giroux).
12. Lev-Yadun, S. (2016). Defensive (Anti-herbivory) Coloration in Land Plants (Springer).
13. Hassanien, R.H., HOU, T.-z., LI, Y.-f., and LI, B.-m. (2014). Advances in effects of sound waves on plants. *J. Integr. Agric.* *13*, 335–348.
14. Gagliano, M., Mancuso, S., and Robert, D. (2012). Towards understanding plant bioacoustics. *Trends Plant Sci.* *17*, 323–325.
15. Tyree, M.T., and Sperry, J.S. (1989). Vulnerability of xylem to cavitation and embolism. *Annu. Rev. Plant Physiol. Plant Mol. Biol.* *40*, 19–36.
16. Cochard, H., Badel, E., Herbet, S., Delzon, S., Choat, B., and Jansen, S. (2013). Methods for measuring plant vulnerability to cavitation: a critical review. *J. Exp. Bot.* *64*, 4779–4791.
17. De Roo, L., Vergeynst, L., De Baerdemaeker, N., and Steppe, K. (2016). Acoustic emissions to measure drought-induced cavitation in plants. *Appl. Sci.* *6*, 71.
18. Zweifel, R., and Zeugin, F. (2008). Ultrasonic acoustic emissions in drought-stressed trees – more than signals from cavitation? *New Phytol.* *179*, 1070–1079. <https://doi.org/10.1111/j.1469-8137.2008.02521.x>.
19. Ikeda, T., and Ohtsu, M. (1992). Detection of xylem cavitation in field-grown pine trees using the acoustic emission technique. *Ecol. Res.* *7*, 391–395.
20. Jackson, G., and Grace, J. (1996). Field measurements of xylem cavitation: are acoustic emissions useful? *J. Exp. Bot.* *47*, 1643–1650.
21. Bailey, N.W., Fowler-Finn, K.D., Rebar, D., and Rodríguez, R.L. (2013). Green symphonies or wind in the willows? Testing acoustic communication in plants. *Behav. Ecol.* *24*, 797–798. [ars228](https://doi.org/10.1111/j.1469-8137.2013.02521.x).
22. ten Cate, C. (2013). Acoustic communication in plants: do the woods really sing? *Behav. Ecol.* *24*, 799–800.
23. Gagliano, M. (2012). Green symphonies: a call for studies on acoustic communication in plants. *Behav. Ecol.* *24*, 789–796. [ars206](https://doi.org/10.1111/j.1469-8137.2013.02521.x).
24. Jung, J., Kim, S.-K., Kim, J.Y., Jeong, M.-J., and Ryu, C.-M. (2018). Beyond chemical triggers: evidence for sound-evoked physiological reactions in plants. *Front. Plant Sci.* *9*, 25.
25. Miller, L.A., and Surlykke, A. (2001). How Some Insects Detect and Avoid Being Eaten by Bats: Tactics and Countertactics of Prey and Predator Evolutionarily speaking, insects have responded to selective pressure from bats with new evasive mechanisms, and these very responses in turn put pressure on bats to “improve” their tactics. *Bioscience* *51*, 570–581.
26. Spangler, H.G. (1988). Moth hearing, defense, and communication. *Annu. Rev. Entomol.* *33*, 59–81.
27. Fullard, J.H., Dawson, J.W., and Jacobs, D.S. (2003). Auditory encoding during the last moment of a moth’s life. *J. Exp. Biol.* *206*, 281–294.
28. Mishra, R.C., Ghosh, R., and Bae, H. (2016). Plant acoustics: in the search of a sound mechanism for sound signaling in plants. *J. Exp. Bot.* *67*, 4483–4494.
29. Jeong, M.-J., Shim, C.-K., Lee, J.-O., Kwon, H.-B., Kim, Y.-H., Lee, S.-K., Byun, M.-O., and Park, S.-C. (2008). Plant gene responses to frequency-specific sound signals. *Mol. Breeding* *21*, 217–226.
30. Ghosh, R., Mishra, R.C., Choi, B., Kwon, Y.S., Bae, D.W., Park, S.-C., Jeong, M.-J., and Bae, H. (2016). Exposure to sound vibrations lead to transcriptomic, proteomic and hormonal changes in Arabidopsis. *Sci. Rep.* *6*, 33370–33417.
31. Veits, M., Khait, I., Obolski, U., Zinger, E., Boonman, A., Goldshtein, A., Saban, K., Seltzer, R., Ben-Dor, U., Estlein, P., et al. (2019). Flowers respond to pollinator sound within minutes by increasing nectar sugar concentration. *Ecol. Lett.* *22*, 1483–1492.
32. Acevedo, M.A., Corrada-Bravo, C.J., Corrada-Bravo, H., Villanueva-Rivera, L.J., and Aide, T.M. (2009). Automated classification of bird and amphibian calls using machine learning: A comparison of methods. *Ecol. Inf.* *4*, 206–214.
33. Giannakopoulos, T., and Piskris, A. (2014). Introduction to Audio Analysis: A MATLAB® Approach (Academic Press).
34. Ellis, D.P. (2005). {PLP} and {RASTA}{and {MFCC}, and inversion} in {M} atlab.
35. Brodrigg, T.J., and Holbrook, N.M. (2004). Diurnal depression of leaf hydraulic conductance in a tropical tree species. *Plant Cell Environ.* *27*, 820–827.
36. Gosa, S.C., Koch, A., Shenhar, I., Hirschberg, J., Zamir, D., and Moshehion, M. (2022). The potential of dynamic physiological traits in young tomato plants to predict field-yield performance. *Plant Sci.* *315*, 111122.
37. Heffner, H.E., and Heffner, R.S. (1985). Hearing in two cricetid rodents: Wood rat (*Neotoma floridana*) and grasshopper mouse (*Onychomys leucogaster*). *J. Comp. Psychol.* *99*, 275–288.
38. Moir, H.M., Jackson, J.C., and Windmill, J.F.C. (2013). Extremely high frequency sensitivity in a ‘simple’ear. *Biol. Lett.* *9*, 20130241.
39. Dutta, S., Chen, Z., Kaiser, E., Matamoros, P.M., Steeneken, P.G., and Verbiest, G.J. (2022). Ultrasound Pulse Emission Spectroscopy Method to Characterize Xylem Conduits in Plant Stems. *Research* *2022*.
40. Khait, I., Sharon, R., Yovel, Y., and Hadany, L. (2020). Plant-monitor. Patent Application Number WO2020039434A1. patent application WO2020039434A1.
41. Playán, E., and Mateos, L. (2006). Modernization and optimization of irrigation systems to increase water productivity. *Agric. Water Manag.* *80*, 100–116.
42. Sadler, E., Evans, R., Stone, K., and Camp, C. (2005). Opportunities for conservation with precision irrigation. *J. Soil Water Conserv.* *60*, 371–378.
43. Allen, C.D., and Breshears, D.D. (1998). Drought-induced shift of a forest-woodland ecotone: rapid landscape response to climate variation. *Proc. Natl. Acad. Sci. USA* *95*, 14839–14842.
44. Specht, A., de Paula-Moraes, S.V., and Sosa-Gómez, D.R. (2015). Host plants of *Chrysodeixis includens* (Walker)(Lepidoptera, Noctuidae, Plusiinae). *Rev. Bras. Entomol.* *59*, 343–345.
45. Liu, Z., Li, D., Gong, P., and Wu, K. (2004). Life table studies of the cotton bollworm, *Helicoverpa armigera* (Hübner)(Lepidoptera: Noctuidae), on different host plants. *Environ. Entomol.* *33*, 1570–1576.
46. Rodrigo-Moreno, A., Bazihizina, N., Azzarello, E., Masi, E., Tran, D., Bouteau, F., Baluska, F., and Mancuso, S. (2017). Root phonotropism: Early signalling events following sound perception in Arabidopsis roots. *Plant Sci.* *264*, 9–15.
47. López-Ribera, I., and Vicient, C.M. (2017). Drought tolerance induced by sound in Arabidopsis plants. *Plant Signal. Behav.* *12*, e1368938. <https://doi.org/10.1080/15592324.2017.1368938>.
48. Jeong, M.-J., Cho, J.-I., Park, S.-H., Kim, K.-H., Lee, S.K., Kwon, T.-R., Park, S.-C., and Siddiqui, Z.S. (2014). Sound frequencies induce drought tolerance in rice plant. *Pak J Bot* *46*, 2015–2020.
49. Gibly, A., Bonshtien, A., Balaji, V., Debbie, P., Martin, G.B., and Sessa, G. (2004). Identification and expression profiling of tomato genes differentially regulated during a resistance response to *Xanthomonas campestris* pv. *Mol. Plant Microbe Interact.* *17*, 1212–1222.
50. Gera, A., Loebeinstein, G., and Shabtai, S. (1983). Enhanced tobacco mosaic virus production and suppressed synthesis of a virus inhibitor in protoplasts exposed to antibiotics. *Virology* *127*, 475–478.
51. Sessa, G., Yang, X.-Q., Raz, V., Eyal, Y., and Fluhr, R. (1995). Dark induction and subcellular localization of the pathogenesis-related PRB-1b protein. *Plant Mol. Biol.* *28*, 537–547.
52. Zinger, E., Gueijman, A., Obolski, U., Ram, Y., Ruby, E., Binder, M., Yechieli, N., Ohad, N., and Hadany, L. (2019). Less fit *Lamium amplexicaule* plants produce more dispersible seeds. *Sci. Rep.* *9*, 6299.

53. Halperin, O., Gebremedhin, A., Wallach, R., and Moshelion, M. (2017). High-throughput physiological phenotyping and screening system for the characterization of plant–environment interactions. *Plant J.* *89*, 839–850.
54. Dalal, A., Bourstein, R., Haish, N., Shenhar, I., Wallach, R., and Moshelion, M. (2019). Dynamic physiological Phenotyping of drought-stressed pepper plants treated with “productivity-enhancing” and “survivability-enhancing” biostimulants. *Front. Plant Sci.* *10*, 905.
55. Dalal, A., Shenhar, I., Bourstein, R., Mayo, A., Grunwald, Y., Averbuch, N., Attia, Z., Wallach, R., and Moshelion, M. (2020). A telemetric, gravimetric platform for real-time physiological phenotyping of plant–environment interactions. *JoVE*, e61280.
56. Andén, J., and Mallat, S. (2014). Deep scattering spectrum. *IEEE Trans. Signal Process.* *62*, 4114–4128.
57. Sifre, L., Kapoko, M., Oyallon, E., and Lostanlen, V. (2013). Scatnet: A MATLAB Toolbox for Scattering Networks.
58. Krivoruchko, K., Goldshtein, A., Boonman, A., Eitan, O., Ben-Simon, J., Thong, V.D., and Yovel, Y. (2021). Fireflies produce ultrasonic clicks during flight as a potential aposematic anti-bat signal. *iScience* *24*, 102194.
59. Schneider, C.A., Rasband, W.S., and Eliceiri, K.W. (2012). NIH Image to ImageJ: 25 years of image analysis. *Nat. Methods* *9*, 671–675.

## STAR★METHODS

### KEY RESOURCES TABLE

REAGENT or RESOURCE	SOURCE	IDENTIFIER
<b>Bacterial and virus strains</b>		
Tobacco Mosaic Virus (TMV)	Gera et al. <sup>50</sup>	N/A
<b>Deposited data</b>		
Recordings of plant sounds	This paper	<a href="https://doi.org/10.5061/dryad.jwstqjqf7">https://doi.org/10.5061/dryad.jwstqjqf7</a>
<b>Experimental models: Organisms/strains</b>		
<i>Solanum lycopersicum</i> ‘Hawaii 7981’	Gilby et al. <sup>49</sup>	N/A
<i>Nicotiana tabacum</i> ‘Samsun NN’	Sessa et al. <sup>51</sup>	N/A
<i>Triticum aestivum</i> (cv fielder)	ICCI	N/A
<i>Zea mays</i> (cv B73)	ICCI	N/A
<i>Vitis vinifera</i> cv Cabernet Sauvignon)	Sdot Hemed nursery	N/A
<i>Mammillaria spinosissima</i>	TAU Botanical Garden	N/A
<i>Lamium amplexicaule</i>	Zinger et al. <sup>52</sup>	N/A
<b>Software and algorithms</b>		
Python version 3.6	Python Software Foundation	<a href="https://www.python.org">https://www.python.org</a>
MATLAB 8.3	The MathWork Inc.	<a href="https://www.mathworks.com/">https://www.mathworks.com/</a>
ImageJ	Schneider et al. <sup>59</sup>	<a href="https://imagej.nih.gov/ij/download.html">https://imagej.nih.gov/ij/download.html</a>
Comsol Multiphysics simulation software	COMSOL	<a href="https://www.comsol.com/">https://www.comsol.com/</a>
MFCC	rastamat	<a href="https://www.ee.columbia.edu/~dpwe/resources/matlab/rastamat/">https://www.ee.columbia.edu/~dpwe/resources/matlab/rastamat/</a>
Scattering networks	scatnet-0.2	<a href="https://www.di.ens.fr/data/software/scatnet/">https://www.di.ens.fr/data/software/scatnet/</a>
LIBSVM: A library for support vector machines	libsvm-3.21	<a href="http://www.csie.ntu.edu.tw/~cjlin/libsvm">http://www.csie.ntu.edu.tw/~cjlin/libsvm</a>
CNN sound classifier	This paper	<a href="https://doi.org/10.5281/zenodo.7612742">https://doi.org/10.5281/zenodo.7612742</a>
<b>Other</b>		
Condenser ultrasound microphones CM16	Avisoft Bioacoustics	<a href="https://www.avisoft.com/ultrasound-microphones/cm16-cmpa/">https://www.avisoft.com/ultrasound-microphones/cm16-cmpa/</a>
UltraSoundGate 1216H A/D converter	Avisoft Bioacoustics	<a href="https://www.avisoft.com/ultrasoundgate/1216h/">https://www.avisoft.com/ultrasoundgate/1216h/</a>

### RESOURCE AVAILABILITY

#### Lead contact

Further information and requests for resources should be directed to and will be fulfilled by the lead contact, Lilach Hadany ([lilach.hadany@gmail.com](mailto:lilach.hadany@gmail.com)).

#### Data and code availability

- Code for the CNN binary classifier training function can be found on Zenodo: <https://doi.org/10.5281/zenodo.7612742>.
- Data including recordings of plants under different conditions can be found on Dryad: <https://doi.org/10.5061/dryad.jwstqjqf7>.
- Additional information can be obtained from the [lead contact](#).

### EXPERIMENTAL MODEL AND SUBJECT DETAILS

*S. lycopersicum* ‘Hawaii 7981’.<sup>49</sup> The plants for the experiments presented in [Figures 1, 2, and 3](#) were grown in a growth room at 25°C and kept in long-day conditions (16 h day, 8 h night). The plants used in the transpiration experiment ([Figure 4](#)) were grown in a greenhouse. The plants used in the infection experiment ([Figure S3F](#)) were grown in a greenhouse and infected with TMV.<sup>50</sup> The plants were tested in the experiments 5–8 weeks after germination.

*N. tabacum* ‘Samsun NN’.<sup>51</sup> The plants were grown in a growth room at 25°C and kept in long-day conditions (16 h day, 8 h night).

*T. aestivum* (cv fielder), grown in a greenhouse.

*Z. mays* (cv B73), grown in a greenhouse.

*Vitis vinifera* (cv Cabernet Sauvignon) grown in a greenhouse.

*Mammillaria spinosissima*, grown in a greenhouse.

*L. amplexicaule*,<sup>52</sup> grown in a growth room, long-day conditions.

## METHOD DETAILS

### Recording protocol

#### In the acoustic box

The recordings were performed in a  $50 \times 100 \times 150 \text{ cm}^3$  acoustically isolated custom-made 1.7cm thick wooden box tiled with 6cm acoustic foam on all sides to minimize echoes. The walls, floor and ceiling of the acoustic box had a maximum Target Strength of  $-40 \text{ dB}$  at 20–30 kHz, dropping off to  $-50 \text{ dB}$  at 65–70 kHz, and the box was located in the quiet basement of the faculty of life sciences TAU, behind thick walls. The box's walls dampened sounds generate outside the box by at least 100 dB SPL in the relevant frequency range (see below details regarding the estimation of the acoustic box acoustics). Two cable holes, 2 cm radius each, were located in two corners of the box and covered with PVC and acoustic foam. Inside the acoustic box were only the recorded plants and 6 microphones connected to an UltraSoundGate 1216H A/D converter (Avisoft). The PC and all the electricity connections were in the room outside the acoustic box. Two USB cables connected the PC to the 1216H device inside the box, through the holes. There was no light inside the acoustic box, and the testing was performed in the dark.

The recordings were performed using a condenser CM16 ultrasound microphone (Avisoft), digitized using an UltraSoundGate 1216H A/D converter (Avisoft), and stored onto a PC. The sampling rate was 500 kHz per channel. We filtered the recordings using 20 kHz high-pass filter. A recording was saved only if triggered with a sound which exceeded 2% of the maximum dynamic range of the microphone. In such cases, a recording of length 1.5 s was saved, starting half a second before the trigger and lasting 1 s after the trigger. Each recording produced a 6-channel wav file (a channel for each microphone). Two microphones were directed at each plant stem, keeping a clear line of sight with no dampening leaves between the stem and the microphones, from a distance of 10 cm. Only sounds that were recorded by both microphones directed at the same plant were considered as “plant sounds” in the analysis afterward. The frequency responses of the microphones can be found in Avisoft website. No sounds were recorded by both microphones from empty pots (with either dry or wet soil), over several weeks of recordings, demonstrating the effectiveness of the box. No sounds were recorded from empty pots even when sharing a box with stressed plants, suggesting that cross talk between microphones was not significant in our setting.

#### In the greenhouse

The recordings were performed in a greenhouse in Tel-Aviv University. During the greenhouse experiment, the only plants that were present inside the greenhouse were the recorded plants. The recordings were performed using the same hardware and setting, as mentioned in the [acoustic box recording](#) section, with three plants in each round and two microphones oriented at each plant, apart from the acoustic box itself.

### Data pre-processing

Data processing was performed offline using python 3.6 code we developed, with the following steps: 1. Identifying the microphone that had recorded the highest intensity peak in each 1.5 s recording file. 2. Selecting only the sounds that were detected by two microphones oriented at the same plant at the same time, and saving the one that triggered the recording for further analysis. 3. Focusing on a short segment of 2ms around the peak. A processed recording includes a segment of 1ms before and 1ms after the peak of a recorded sound that triggered the system to record. “Greenhouse noise” sounds were obtained when the greenhouse included only acoustic equipment without plants or pots, by the two microphones (thus excluding “Electrical noise” registered on a single microphone).

### Acoustic-box drought stress experiment

Each plant was recorded twice: first before drought treatment (“self-control”), and again after it. In the first recording, all the plants were healthy and their soil was moist. Then, for 4–6 days, half of the plants were watered while the other half were not, until the soil moisture in the pots of un-watered plants decreased below 5%. Then, the plants were recorded again at the same order. In each recording session three plants were recorded simultaneously for 1 h and each triplet of plants included at least one watered and one un-watered plant to allow “neighbors-control” – watered plants that were recorded while sharing the acoustic box with un-watered plants. Soil moisture content was recorded using a hand-held digital soil moisture meter - Lutron PMS-714.

### Acoustic-box cut stress experiment

The experiment followed the experimental design of the drought stress experiment described above, but drought stress was replaced with cutting of the plant. Here the pot soil was kept moist for all the plants throughout the experiment. The plants included in the treatment group were cut with scissors close to the ground right before the recording started. The severed part of the plant, disconnected from the roots, was recorded. We used the same controls of the drought stress experiment.

### Greenhouse drought experiment

In each recording session three plants were recorded simultaneously for 1 h. All the recorded plants were grown in a growth room, and were brought to the greenhouse only for the recording session. Each plant was recorded either one day after irrigation (control plants) or 4–6 days after irrigation (drought-stressed plants). The results of that experiment are presented in [Figure 2](#).

### Greenhouse dehydration experiment

In each recording session three plants were recorded simultaneously for several consecutive days without watering. All the recorded plants were grown in a growth room, and were brought to the greenhouse only for the recording session. In addition, the soil of each plant was monitored every 30 min throughout the experiment, using Decagon GS3 sensors. The results of that experiment are presented in [Figure 3](#).

### Greenhouse whole plant transpiration rate

Whole-plant physiological performance was monitored with the functional phenotyping system [Plant-Ditech platform](#).<sup>53</sup> The [Plant-Ditech system](#) was calibrated before the experiment start, and 5–7 weeks old plants were used for measurements (same as for the drought and dehydration experiments). Plants were measured along several consecutive days without watering. The transpiration rate (TR) of the plants during the course of the experiment were determined using standard previously described protocols.<sup>53–55</sup> The results of that experiment are presented in [Figure 4](#).

### Classifying sounds recorded in the acoustic box

Our classification method was composed of two main stages. First, we extracted various acoustic features from the raw recorded signals (see [data Pre-processing](#) section). Second, we trained a model to classify plant sounds into classes based on the feature representation obtained in the first stage. A separate model was trained for each comparison. We used three methods of feature extraction: (a) Deep scattering Network, as described in Andén and Mallat<sup>56</sup> (red dotted line in [Figure 1F](#)). This method extends MFCC (Mel-frequency cepstral coefficients) while minimizing information loss. We used the implementation by ScatNet,<sup>57</sup> with Morlet wavelets. The results were robust to the dimension of descriptors and the scattering network specific parameters: number of layers used; time support of low pass filter; and Q-Factor ([Figure S1D](#)). The values of the specific parameters used in this work are shown in [Table S2](#). (b) MFCC feature extraction (dashed black line in [Figure 2B](#)). We used the Dan Ellis implementation.<sup>34</sup> (c) Basic features. The basic features we used were energy, energy entropy, spectral entropy, and maximum frequency (gray line in [Figure 1F](#)).<sup>32,33</sup> We used SVM with Radial kernel with the LIBSVM implementation as classifier. After feature extraction, we used Z score for normalization of the features and PCA to reduce the dimensionality of the problem. We conducted LOPO-CV examination for evaluation of model accuracy (see below).

We repeated the analysis using binary CNN models (see below), over either raw sound vectors or sound vectors normalized for intensity (by dividing each value by the vector's maximal value), with similar levels of accuracy ([Figure S1E](#)). The numbers of plants in each group are shown at the [Table S3](#).

### Convolution neural networks (CNN)

For the implementation of convolution neural networks we used Python 3.6 with keras package and tensorflow backend. All of the CNN models presented in this manuscript (except for the analysis in [Figure S3E](#)) are based on the same network architecture. The network is composed of three blocks, each including two 1D convolution layers with a 'relu' activation, followed by a maxpooling layer and a dropout layer. These three blocks are followed by one fully-connected layer with 'relu' activation and another dropout layer. At the end, we add a fully-connected layer of size 1 with sigmoid activation. The model is trained for 50 epochs with binary 'crossentropy' loss function and 'adam' optimizer.

For the analysis presented in [Figure S3E](#) (3-categories classification) we replace the last layer (of size 1 with sigmoid activation) by a fully-connected layer of size 3, with 'softmax' activation. This model is trained with 'categorical\_crossentropy' loss function.

### Leave-one-plant-out cross validation (LOPO-CV)

In order to obtain robust evaluations of the models we trained, and to verify that individual differences between plants do not drive the results, we conducted leave-one-plant-out cross validation (LOPO-CV) examinations throughout the paper. In each step of the CV, we left all of the emitted sounds of one plant for testing, and used the rest of the sounds for training. We repeated this process so that each plant was used for testing exactly once. This, the number of CV steps is equal to the number of plants in the analysis. For each CV, we then constructed a confusion matrix by summing all of the accurate and wrong predictions. We sum all these matrices to obtain one confusion matrix that summarizes the success from the entire CV process, from which we derived the balanced accuracy score.

When one of the examined groups is of noises (either electric noises or greenhouse noises), where the sounds are not emitted by plants, we randomly split the sounds into several groups that will be used for the CV. For examination of the SVM models, in each CV step we constructed a training set, including two groups of equal size, by randomly omitting samples from the larger group.

### Classifying sounds recorded in the greenhouse

For classification of greenhouse noises and drought-stressed tomato sounds, we used a convolution neural network (see CNN section above). We first examined the performance of the CNN models on our sound libraries: dehydrated tomato sounds from the acoustic box and empty greenhouse noises, applying LOPO-CV. This analysis yielded a balanced accuracy score of 99.7%.

We repeated the evaluation analysis with two forms of normalization: (a) for sound intensity (by dividing each value in the sound vector by the vector's maximal absolute value); (b) for background noise, by superimposing each sound vector obtained from the acoustic box on a randomly chosen background sound from the greenhouse and each sound from the greenhouse on a randomly chosen background sound from the acoustic box (see Figure S2B for illustration). The results were very similar and highly significant after these two corrections.

For the application of the CNN model on sounds recorded in the greenhouse experiments (including Figures 2D, 3, 4), classifying each sound as either a tomato sound or a greenhouse noise, we trained a CNN model over the entire libraries of dry tomato sounds (from the acoustic box) and empty greenhouse noises.

### Estimation of the animal detection range

The distance at which a moth/mouse would detect the clicks produced by a tomato plant was calculated using the sound propagation equation:  $cSPL - 20 \cdot \log_{10}(R/R1) - \alpha(R-R1) + \log_{2.7} = HT$ , where HT is hearing threshold of a moth or a grasshopper mouse (set to 35 and 10 dB SPL Re 20  $\mu$ Pa respectively<sup>37,38</sup>), cSPL is the mean emitted plant sound pressure level set to 65 dB SPL based on our recordings. R is the detection distance (m), R1 is the recording distance of the plant and  $\alpha$  is a frequency dependent atmospheric attenuation factor (1.6 dB/m at the most intense emission frequency) for the average temperature and humidity levels in the area (26°C at night and 80% respectively). Note that some researchers argue that HT should be 10 or even 0 dB SPL Re 20  $\mu$ Pa in which case the detection range would further increase, but we preferred an underestimate to be on the safe side.

### Microphone calibration

The Avisoft CM16 microphone's sensitivity is 500 mV/Pa and is almost flat between 10 and 120 kHz (see <http://www.avisoft.com/ultrasound-microphones/cm16-cmpa/>). The sensitivity of the microphones used in this experiment were calibrated using a calibrated GRAS (40DP) microphone by emitting signals covering the relevant frequency range toward the two microphones when positioned at the same distance relative to the speaker. For playback, an ultrasonic speaker (Vifa, connected to an Avisoft 116 D/A converted) was used to play back sound sweeps in the relevant frequency range (1 ms tones at frequencies between 70 and 20kHz). This procedure is routinely used in the lab for various acoustic measurements (see e.g.,<sup>58</sup>). Our GRAS microphone is routinely calibrated using a Larson Davis CAL150 calibrator with a 1kHz 94 dB SPL calibration tone. The CM16 microphone is much more directional than the GRAS so its calibration is accurate only when the sound is arriving on-axis. CM16 directionality can be found here (<http://www.avisoft.com/ultrasound-microphones/cm16-cmpa/>). Our sound intensity estimates are thus a lower bound on the actual intensity.

### Estimating the acoustic box properties

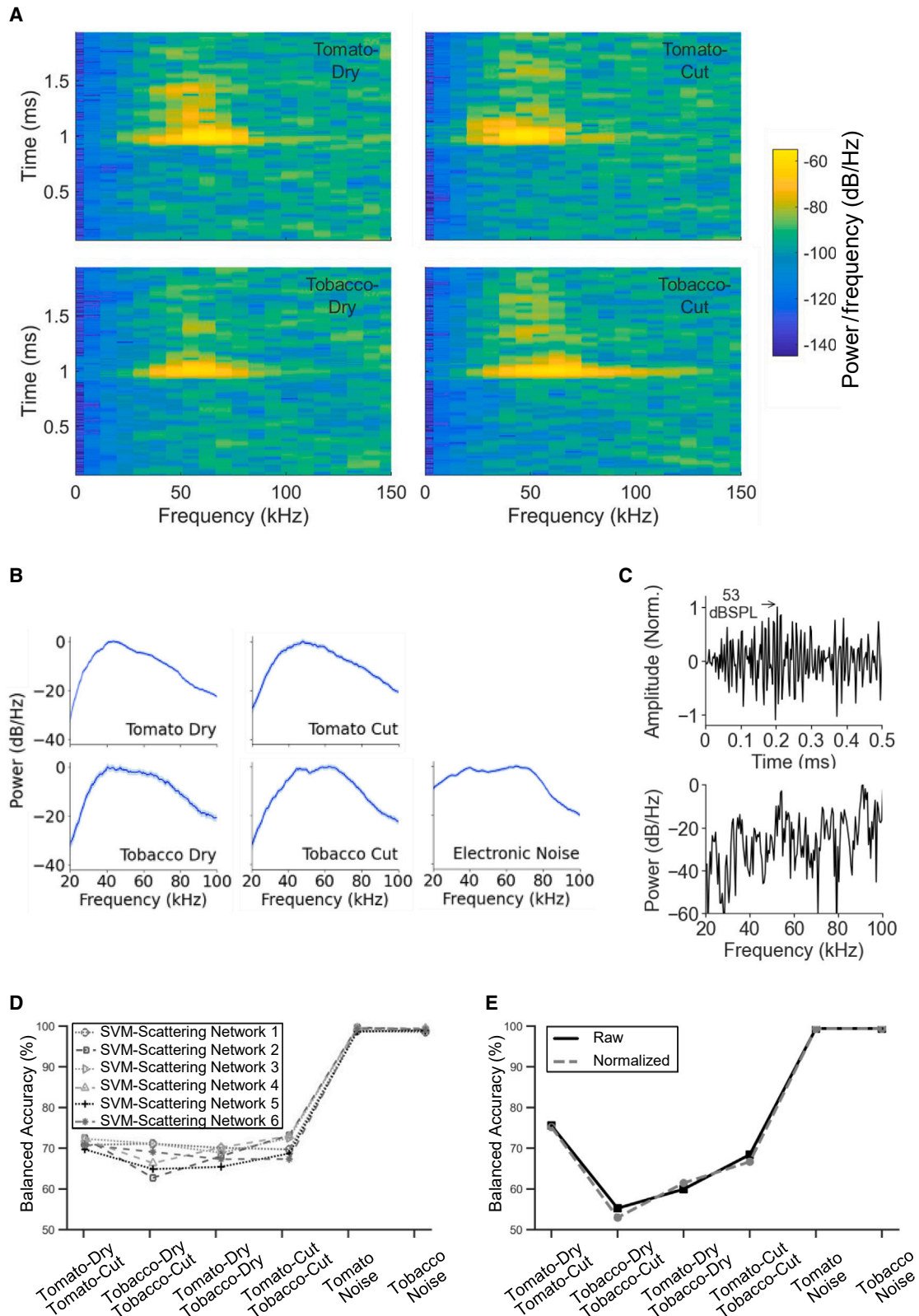
The echoic properties of the chamber were measured by playing a 70 to 20 kHz pulse of 1 ms duration through a Vifa loudspeaker with a loudness of 116 dB SPL at 30 kHz. The foam at a distance of 93 cm from the speaker received 97 dB SPL, resulting in strongest echoes of 57 dB SPL at 30 kHz with virtually no energy visible above 40 kHz. Absolute sound pressure levels from the loudspeaker were measured by a GRAS instrumentation microphone 40DP connected to an Hm116 Avisoft sampling board, sampling at 375 kHz. Echoes were measured with same CM16 microphone used in the plant data acquisition. The GRAS instrumentation microphone was calibrated during the measurements using a Larson Davis CAL150 calibrator with a 1kHz 94 dB SPL calibration tone.

Clapping of 100 dB SPL right outside the box remained under the noise floor measured inside the box >20kHz. Also, speaker playbacks of 116 dB SPL of 70 to 20 kHz pulses failed to trigger the system and when the system was triggered manually did not lead to any energy above the noise floor.

## QUANTIFICATION AND STATISTICAL ANALYSIS

For statistical analysis of the number of sound emissions for the treatment and the control groups (Figure 1F) we used the Wilcoxon rank-sum test. To compare our classifier to random result (Figure 2B), we used the binomial probability distribution function (PDF) and calculate the probability to get the classifier accuracy or higher randomly for each group. To compare the results obtained when using scattering network<sup>26</sup> for feature extraction to the results obtained when using MFCC<sup>34</sup> or basic feature<sup>29,30</sup> extraction methods (Figure 1F), we used Wilcoxon sign rank test with Holm-Bonferroni correction. To test the success in distinguishing between drought-stressed and control plants (Figure 2) we used Fisher's exact test. To test the differences in the number of emitted sounds per day (Figure 3A) we used Wilcoxon signed-ranks tests with Holm-Bonferroni adjustment for multiple comparisons.

# Supplemental figures



---

**Figure S1. Plant sounds recorded in the acoustic box, related to Figure 1**

(A) Plant sound spectrograms. Spectrograms of sounds emitted by stressed plants: a drought stressed tomato, a drought stressed tobacco, a cut tomato and a cut tobacco. The corresponding time signals and spectra of these sounds are shown in [Figures 1C and 1D](#).

(B) Mean spectra of the sounds recorded in the acoustic box. Average signal spectrum of five groups of normalized sounds: Emitted by dry tomatoes, cut tomatoes, dry tobacco, cut tobacco, and electronic noise. The light blue areas around the line represent the standard error of the mean.

(C) Example of electronic noise. Top—time signal of the noise, normalized to the peak. Bottom—spectrum of the sound shown above. The electronic sound was recorded in the acoustic box, but only by one microphone, and was thus not considered as “plant sound” for further analysis.

(D) Comparison of different scattering network configurations. The accuracy of sound classification with 6 different configurations for the scattering network, using SVM as classifier. Each line represents a different feature set, all obtained by scattering network. The scattering networks had different time intervals, different Q-factors, and a different number of filters, for exact values see [Table S1](#).

(E) The accuracy of sound classification achieved by CNN models. The balanced accuracy of sound classification achieved by binary CNN models (see [STAR Methods](#)), for training and testing on the raw sound-vectors (black) and for training and testing on sound-vectors that were normalized by dividing each value in a vector by the vector’s maximal absolute value. Each balanced accuracy result is based on leave-one-plant-out cross validation (LOPOCV, see [STAR Methods](#)).



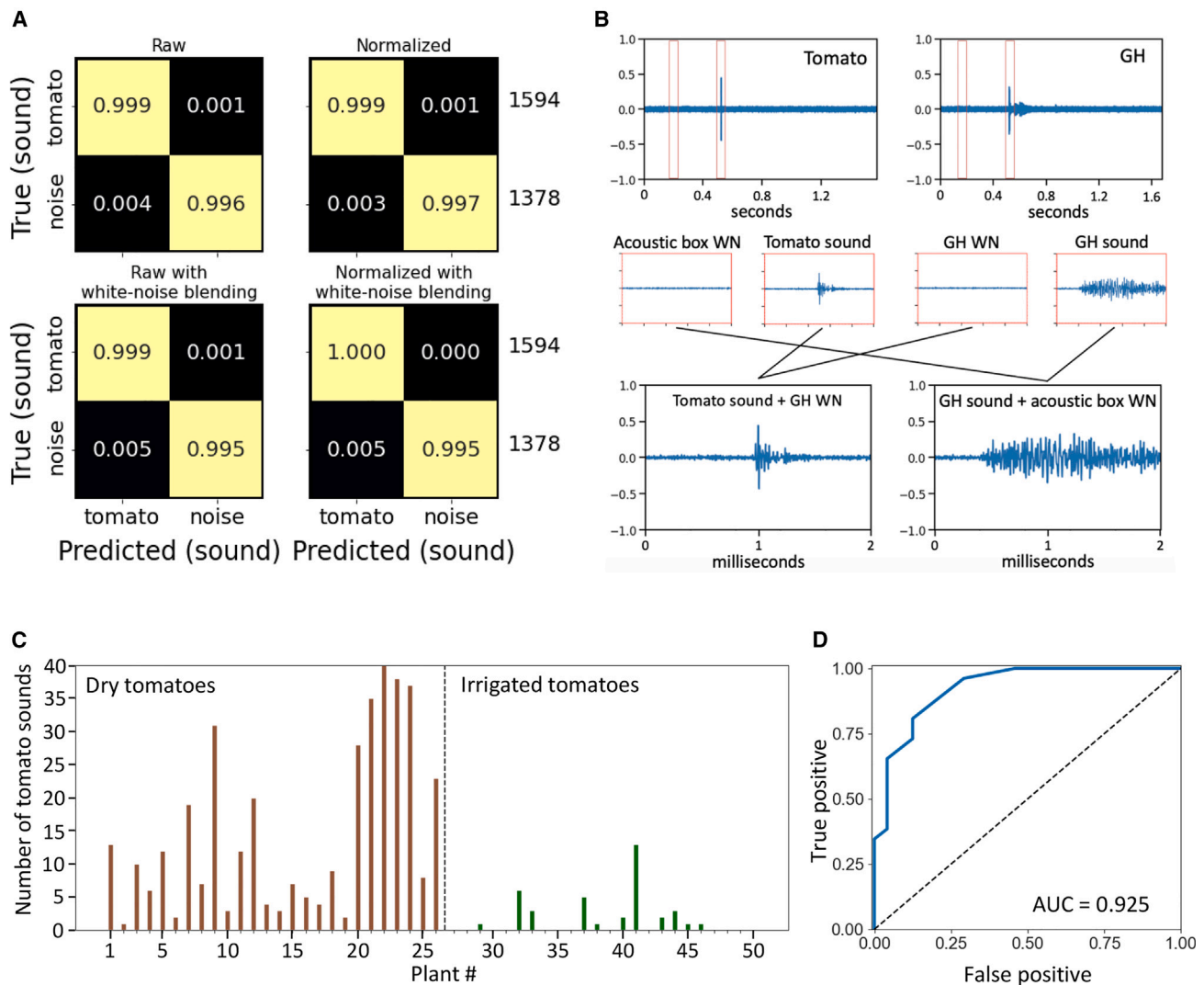


**Figure S2. Analysis of plant sounds recorded in the greenhouse, related to Figure 2**

(A) Success of CNN models in distinguishing between tomato sounds and greenhouse (GH) noises. Confusion matrices showing the success of trained CNN classifiers in distinguishing between tomato sounds and GH noises, with different corrections: raw sound-vectors (upper-left), sound vectors that were normalized by dividing each value in a vector by the vector's maximal absolute value (upper-right); raw sound vectors that were super-imposed with raw white noise vectors (WN) from the opposite group (tomato sound + white noise from the GH, GH sound + white noise from the acoustic box, lower-left); normalized sound vectors that were super-imposed with a normalized white noise vector from the opposite group (lower-right). These confusion matrices are the summation of the confusion matrices that are produced in the LOPOCV process (see STAR Methods).

(B) Illustration of the construction of super-imposed sounds. First, libraries of white noises (WN) from the acoustic box and from the greenhouse are generated, by taking ten 2ms segments from the time segment 200-400ms of each sound from the dry tomato library (acoustic box) and from the empty greenhouse noises. These selected segments appear 100-300ms before the signal that triggered the recording (see STAR Methods in the main text), and they contain white noises characteristic to the recording environment. We then generate super-imposed sounds, by summing (element-wise) the tomato sound vectors, each with a randomly selected greenhouse white noise vector, and by summing the greenhouse sounds, each with a randomly selected acoustic box white noise vector. After the summation we trim the vectors so that all values greater than 1 are set to 1, and all values smaller than -1 are set to -1.

(C) Tomato-classified sounds per hour. We recorded dry and irrigated tomato plants for 1 h in the green house. Then, using a trained Convolutional Neural Network (CNN) we filtered the greenhouse noises and left only the tomato classified sounds. We here show the number of tomato-classified sounds, recorded during 1 h in the greenhouse for dry and irrigated tomato plants. The y axis is truncated at 40 for better resolution; plant 22 emitted 95 sounds.

(D) Receiver operating characteristic (ROC) curve presenting the performance of the classification model used to distinguish between dry and irrigated tomato plants. We plot the true positive rate as function of the false positive rate for all possible decision threshold, where a decision threshold is of the type: above a certain number ( $n_c$ ) of tomato-classified sounds per hour we classify the plant as dry, otherwise we classify the plant as irrigated.

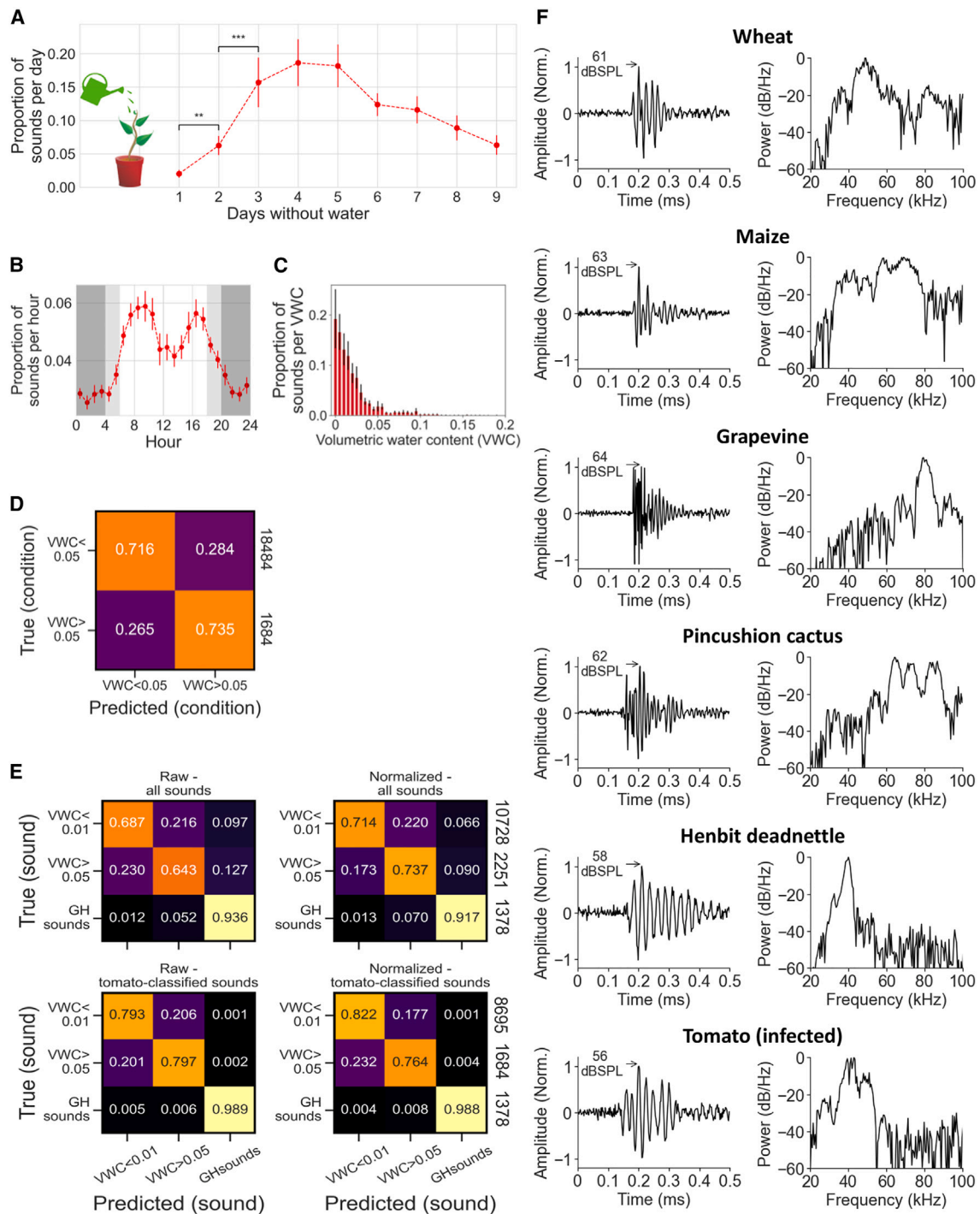


**Figure S3. Acoustic manifestations of dehydration and other stress factors in multiple plant species, related to Figure 3**

(A) The proportion of sounds per day along nine consecutive days of dehydration in tomato plants. The dots represent the average of 23 plants, while the error bars represent the standard errors. We find significant differences in the proportion of emitted sounds between the first and second day, and between the second and third day ( $p$  values are  $<0.01$  and  $<0.001$  respectively;  $p$  values were calculated using Wilcoxon signed-ranks tests, adjusted for 8 comparisons between pairs of consecutive days using Holm-Bonferroni method). The soil volumetric water content (VWC) of the plants at the beginning of the recording was  $0.21 \pm 0.03$  ( $m^3/m^3$ ; mean  $\pm$  std).

(B) The proportion of sounds per hour is plotted as a function of the time of day. Each dot represents the average proportion of sounds emitted in the relevant hour over all 23 plants and nine days, while the error bars represent the standard errors. Dark gray areas represent the hours of complete darkness, light gray areas show when the greenhouse lighting was on, and the white area represents the approximate hours of natural daylight.

(legend continued on next page)

---

(C) A bar plot showing the proportion of emitted sounds as a function of the plant VWC during sound emission. The bars present the averages of the 23 plants, while the bars represent the standard errors.

(D) Confusion matrix showing the success of the trained CNN classifiers (see [STAR Methods](#)) in distinguishing between sounds emitted by a plant experiencing  $VWC < 0.05$  and sounds emitted by a plant experiencing  $VWC > 0.05$ , in a LOPOCV process (see [STAR Methods](#)). The balanced accuracy score is 72.5%.

(E) The success of CNN models in distinguishing between sounds emitted by tomato plants with low and higher VWC values without pre-classification. Confusion matrices showing the success of CNN classifiers in distinguishing between sounds that are linked to a plant experiencing  $VWC < 0.01$ , sounds that are linked to a plant experiencing  $VWC > 0.05$  and sounds recorded in an empty greenhouse (GH sounds). The analysis in all four sub-panels is based on the recordings of the multi-day experiment ([Figure 3](#)). The recorded sounds (either emitted by a plant, or greenhouse noises) were tagged according to the VWC of the plant at the time of the sound emission. These sounds, along with the empty GH sounds library, were fed to 3-class CNN classifiers. Four pre-processing procedures were used, and a confusion matrix was calculated for each procedure, while applying LOPOCV process (see [STAR Methods](#)): all sounds from the GH experiment were included and the raw sound vectors were used (upper-left); all sounds from the GH experiment were included and the sound vectors were normalized (upper-right); sounds from the GH plant-recordings were pre-classified by our CNN, and only sounds classified as tomato sounds were used, as raw sound vectors (lower-left); sounds from the GH plants-recordings were pre-classified by our CNN, and only sounds classified as tomato sounds were used. All the sounds were normalized (lower-right). (F) Examples of recorded sounds from different plants. Left - Examples of time signals of 6 plants (top to bottom): *Triticum aestivum* (Wheat, dry), *Zea mays* (Corn, dry), *Vitis vinifera* (Grapevine, Cabernet Sauvignon variety, cut), *Mammillaria spinosissima* (Pincushion Cactus, cut), *Lamium amplexicaule* (Henbit deadnettle, cut), and *Solanum lycopersicum* (Tomato, infected with TMV). Right - Spectra of the sounds on the left, normalized. Each of these plants emitted a significant amount of sounds when stressed, suggesting that sound emission is common under stress among non-woody plants. We have not succeeded recording from woody plants (almond tree, woody parts of grapevine) using our methodology.

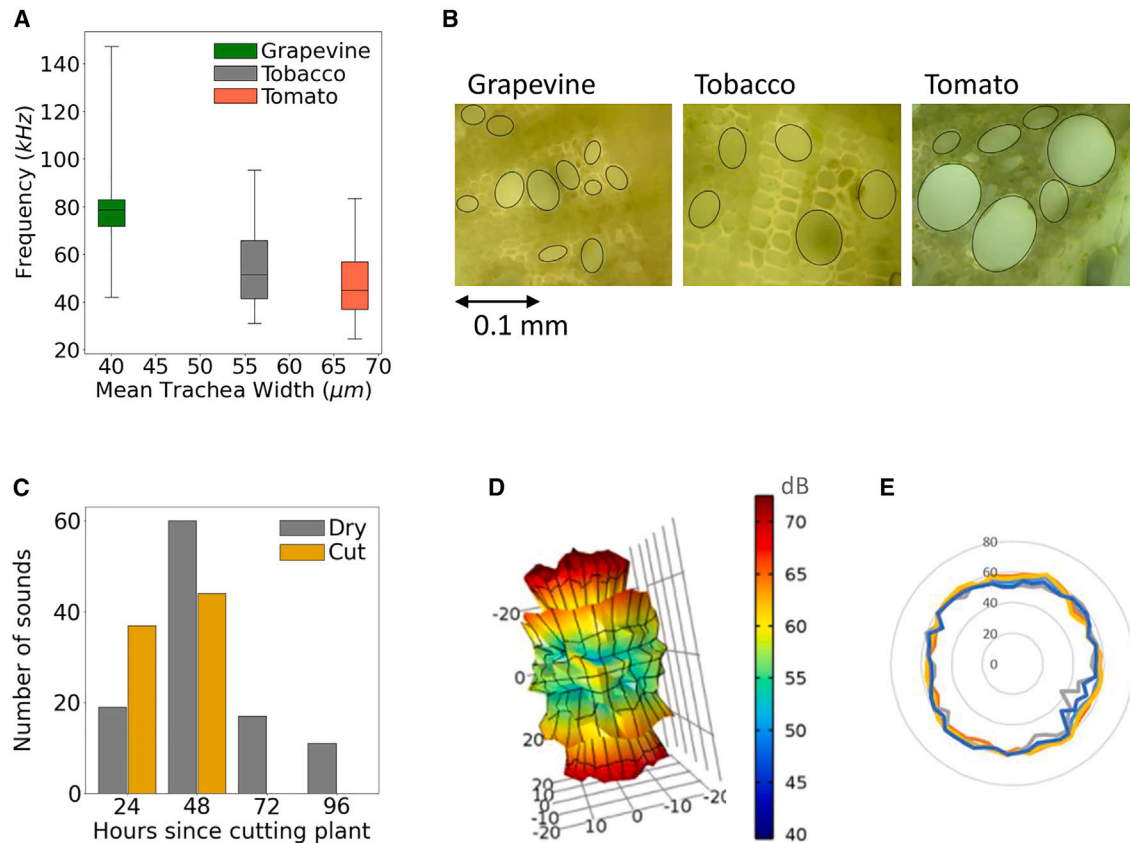


**Figure S4. Additional investigation of the mechanism of plant sound emission, related to Figure 4**

(A) Sound frequency and trachea cross-section width. Boxplots of the distribution of the plant's max frequencies vs. its tracheas' cross section width (estimated as the average of the ellipse width and height, see examples below) for grapevine, tobacco, and tomato.

(B) Examples of three photos used for the estimation of trachea dimensions. Grapevine (Left) Tobacco (middle), and tomato (right). We performed horizontal cross section of tomato, tobacco and grapevine stems to measure their trachea cross section area from pictures taken under the microscope, as shown, using ImageJ.<sup>59</sup>

(C) Classification of sounds emitted by plants that experienced both dehydration and cutting. The sounds emitted by cut-and-dry plants in the acoustic box were classified as either "cut" or "dry". We see that while the overall fraction of sounds classified as "dry" in that experiment is around 55%, it varies with time: right after cutting, sounds classified as "cut" are more common, but from day 2 the majority of sounds are classified as "dry".

(D) Comsol simulations demonstrating sound propagating in all directions from within a stem-like structure. Presented is the 3D far-field sound field.

(E) Horizontal cross section through the sound field from (D) (different colors show different heights along the stem). The simulation shows that sound spreads equally in all directions in the horizontal plane. The virtual model included two concentric silicon tubes (3.6cm diameter and 4 cm diameter) representing the xylem vessels within the stem. Because the size was ca. 10 times larger than a real plant, we used a frequency ca. 10 times lower – 7500Hz, thus maintaining the ratio similar to the real plant. The length of the stem model was 45cm to avoid any effects of length.